ASPS Conference Proceedings 1: 1129-1137 (2022)

Proceedings of

12th Structural Engineering Convention-An International Event (SEC 2022)

Available at https://asps-journals.com/index.php/acp

# Seismic Performance of Coupled Buildings Connected by Yield and SMA Dampers

P. Singh [1], S. Gur [2,*], K. Roy [3]

[1] Department Civil and Environmental Engineering, Master Degree Student, Indian Institute of Technology Patna, Bihta, Patna-801106, India
[2,3] Department Civil and Environmental Engineering, Assistant Professor, Indian Institute of Technology Patna, Bihta, Patna-801106, India

**Paper ID - 070456**

## Abstract

Efficient attenuation and control of structural vibration during a seismic event is a critical factor for overall safety and serviceability of the adjacent buildings with little clearance between them. Without proper vibration control measures, adjacent buildings may undergo severe pounding and collapse leading to damage of life and property during an earthquake. Use of energy dissipation devices to connect adjacent buildings has been a popular method of vibration control and to stop mutual poundings. Among various available energy dissipation devices, Shape Memory Alloy (SMA) based dampers are getting popularity in recent time. Various studies are performed to show the efficiency of SMAs as passive vibration control device, but a holistic study of SMA dampers for non-linear connected buildings is still missing. Thus, here a comparative study on the efficiency of metallic yield and super-elastic SMA dampers as passive vibration control device is provided, for non-linear connect buildings. In the present study, non-linear dynamic time history analyses are performed to determine the response (peak floor acceleration and displacement, and floor residual displacement). Time history analyses confirm better acceleration and displacement (both peak and residual) control efficiency of SMA dampers over yield dampers. Finally, superiority of the SMA damper over the yield damper is established via parametric study under varying damper, building and ground motion parameters. Over yield damper, SMA damper reduces acceleration by 13 % to 56 %, displacement by 2 % to 47 %, and residual displacement by 15 % to 64 %.

*Keywords*: Non-linear Connected Building, Yield Damper, SMA Damper, Seismic Loading, and Passive Vibration Control

## 1. Introduction

It has been found during the past seismic events, mutual pounding [1–4] is the most devastating reason for the collapse of adjacent buildings. Rapid population growth and limited availability of the land around crowded city centres has led to the development of high-rise buildings with little or no spacing in between, increasing the risk of pounding of these buildings. Therefore, for many years, structural engineers have been working actively to mitigate the risks of mutual poundings and to increase the overall safety of the adjacent buildings. One of the popular method adopted is mechanical separation of the buildings using an energy dissipation device. For this purpose, various active, passive and semi-active vibration control devices [5–8] or dampers are being used. Thus, novel better materials and devices are constantly being searched. Among the three broad categories of the control devices, passive dampers work without any external monitoring, power and control system hence are the most popular then other two systems. Energy dissipation and vibration control in these devices are actuated by the relative movement of various points of the structure used to connect the dampers.

Some popular vibration control devices currently in use are the yield dampers, viscoelastic dampers, viscous dampers and the friction dampers. Here, yield and friction dampers [2, 3, 9] show good control efficiency and dissipate significant amount of the seismic energy coming to the structures, but lacks strain recovery after removal of the loads. Thus, they leave large residual displacements and permanent offsets in the structure after a seismic event. Past studies on viscoelastic dampers [1, 4] shows its effective seismic response control efficiency of building structure, via providing supplemental damping. But performance of viscoelastic dampers is strongly affected by variations in temperature, excitation frequency and shear strain, making its designing complex. Also, there are concerns about the stiffness deterioration of these dampers with time. Fluid viscous dampers [8, 10–13] and the viscous inertial mass dampers [14] shows good seismic control efficiency for the connected buildings, but provide poor durability, leading to higher maintenance cost. Therefore, a strong need of passive damping system exists which is convenient to install and maintain, durable in long run, shows good energy dissipation with significant strain recovery after removal of the seismic loads. As a result, Shape memory alloys (SMAs) are getting popularity as a suitable material for passive damping devices in recent years [15]. SMAs shows (a) good energy dissipation through flag shaped hysteresis loops (super-elasticity), and (b) the negligible residual displacement (shape memory effect), making it a suitable material for application in the

*Corresponding author. Tel: +91-6115233819; E-mail address: sgur@iitp.ac.in





Published online: December 19, 2022
doi:10.38208/acp.v1.632

vibration control devices. Studies suggested that SMAs are durable, corrosion and fatigue resistant [16] in long-run.

Previous studies [1, 2, 4, 11] on connected buildings with various types of passive dampers considers buildings will remain in linear regime. This approximation gives satisfactory results when ground motions used in the study are not severe and dampers dissipate the incoming seismic energy[8], limiting buildings in linear range. But a study incorporating non-linearity of the coupled buildings will add much needed clarity. Also, buildings are expected to behave non-linearly under severe ground motions and this paper discusses response of connected buildings under scaled ground motions later, making it compulsory to consider the non-linear behaviour of the buildings.

The present paper primarily focuses on examining the superior control efficiency of the SMA damper over the yield damper for connecting two adjacent and non-linear buildings. As discussed, one of the key points in this study is that, the numerical models capture the non-linearity of the buildings which are modelled using non-linear Bouc-Wen material model for steel. First a non-linear dynamic time history analysis is performed to study the response time history (acceleration and displacement) of the buildings under selected real ground motion data. Finally, dampers, buildings, and ground motion parameters are varied to study their effect on response control efficiency of the yield and SMA dampers for the connected buildings.

## 2. Material Modeling of Building and Dampers

This section discusses the material modelling details of the connected buildings, yield dampers and SMA dampers. In the present study, buildings are modelled to capture the non-linearity and dampers are also modelled considering non-linear material properties as discussed below.

### *2.1 Bouc-Wen Material Model*

Fig. 1 shows the bi-linear force-displacement curve to depict the bi-linear hysteresis loop of the building and yield damper, as modeled via Bouc-Wen material model [17]. These hysteresis loops dissipate a significant part of input energy. This model successfully simulates the non-linear force deformation characteristics of steel material and is expressed in Eq. 1 and 2.

$$F_z(x, Z) = \alpha_z k_z x + (1 - \alpha_z) F_{yz} Z \quad (1)$$

$$\dot{Z} = \left(\frac{\delta}{q_z}\right)\dot{x} - \left(\frac{\gamma}{q_z}\right)|\dot{x}|Z|Z|^{\eta-1} - \left(\frac{\beta}{q_z}\right)\dot{x}|Z|^{\eta} \quad (2)$$

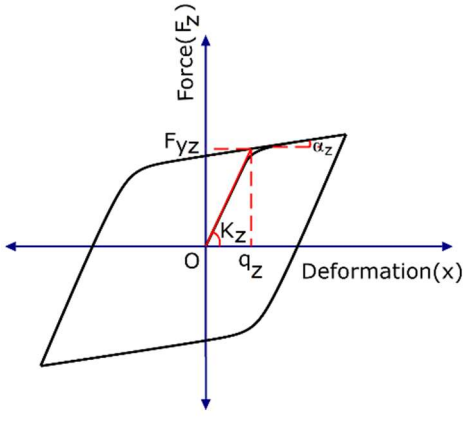


**Fig. 1:** Bouc-Wen Force-Deformation model

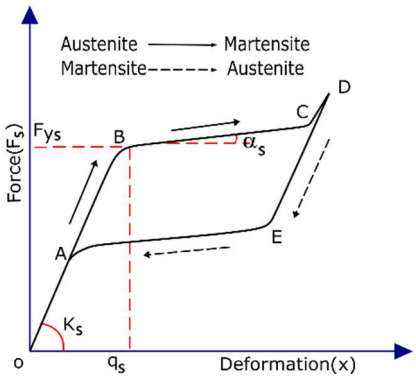


**Fig. 2:** Graesser-Cozzarelli Force-Deformation model

Here, $F_z$ is the restoring force, $k_z$ represents the initial elastic stiffness, $\alpha_z$ is the post to pre yield stiffness ratio (i.e., rigidity ratio), $F_{yz}$ is the yield strength and $q_z$ is the displacement, $x$ the relative displacement, and $\dot{x}$ is the relative velocity, the variable $Z$ is the non-dimensional parameter, represents the hysteretic behavior of a metallic material such as steel. Finally, parameter $\delta, \gamma, \beta$ and $\eta$ controls the shape and transition (elastic to plastic) of the hysteresis loop.

### *2.2 Graesser-Cozzarelli Material Model*

Two important characteristics of SMA are shape memory effect (SME) and super-elasticity (SE). Fig. 2 shows a flag-shaped force-deformation behaviour of super-elastic SMA, as modelled via Graesser-Cozzarelli (GC) constitutive relation[18]. Also. Fig. 2 shows SMA's hysteresis loop is big enough for significant energy dissipation, as well as it has almost no residual displacement after unloading. 1-D form of GC material model is expressed in Eq. 3 and 4.

$$\dot{F}_s(\dot{x}, \beta) = k_s\left[\dot{x} - |\dot{x}|\left|\frac{F_s - \beta}{F_{ys}}\right|^{(v-1)}\left(\frac{F_s - \beta}{F_{ys}}\right)\right] \quad (3)$$

$$\beta = \alpha_s k_s\left[x - \left(\frac{F_s}{k_s}\right) + \frac{2 f_T |x|^c}{\sqrt{\pi}}\int_0^{ax} e^{-a^2x^2} d(ax)\right] \quad (4)$$

Here, $F_s$ is the restoring force of SMA spring, $k_s$ is the initial stiffness of SMA in Austenite phase, $\alpha_s$ is the ratio of pre to post transformation stiffness, $F_{ys}$ and $q_s$ are the forward-transformation strength and displacement for the Austenite to Martensite phase conversion, $x$ and $\dot{x}$ are the relative displacement and velocity, $\eta$ controls the sharpness of the loop, and $\beta$ represents the 1-D back stress. Parameter $a, c$, and $f_T$ controls the amount of recovery, slope of unloading path, and type and size of hysteresis loop, respectively.

## 3. Analysis and Simulation Process

Details of the analysis and simulation is provided in this section. It covers the formulation of equation of motion of the coupled non-linear building-damper system and the ground motion details.

### *3.1 Numerical Modeling*

For numerical simulation, buildings are considered to be 2-D steel frames idealized as non-linear shear buildings. One of the building is seven storey flexible building and other one is five storey stiff building, as adopted in this study. Non-linear Bouc-Wen material model is used in modelling of these

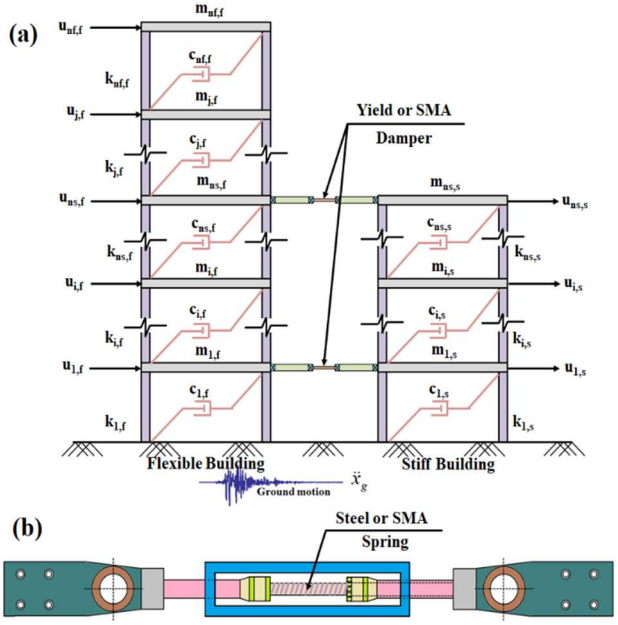


**Fig. 3:** (a) Idealized model of connected building structures and (b) mechanical model of yield/SMA damper.

buildings. Both the buildings are connected at alternate floor levels starting from first floor (i.e., at 1st, 3rd, and 5th floor) once with Yield damper and then with SMA damper. Yield and SMA dampers behaves non-linearly and is modelled using Bouc-wen and Graesser-Cozzarelli material model. Fig. 3 (a) and (b) shows the idealized model of the buildings connected via those dampers and the mechanical model of the dampers, respectively.

Considering buildings as well as dampers to be non-linear, on the basis of force equilibrium following equations can be derived for the coupled-building damper system.

$$[M_f]\{\ddot{u}_f\} + [C_f]\{\dot{u}_f\} + [K_f]\{u_f\} + [F_{fhb}]\{z_f\} + \{F_{hf}\} = -[M_f]\{r_f\}\ddot{u}_g \quad (5)$$

$$[M_s]\{\ddot{u}_s\} + [C_s]\{\dot{u}_s\} + [K_s]\{u_s\} + [F_{shb}]\{z_s\} + \{F_{hs}\} = -[M_s]\{r_s\}\ddot{u}_g \quad (6)$$

Here $[M]$, $[C]$ and $[K]$ are the mass, damping and stiffness matrices respectively, the subscript $'f'$ denotes flexible building and $'s'$ corresponds to the stiff building. Similarly $\{u\}$, $\{\dot{u}\}$ and $\{\ddot{u}\}$ are the displacement, velocity and acceleration of each floor of flexible and stiff building, respectively. $[F_{fhb}]$ and $[F_{shb}]$ are non-linear hysteresis force matrix for flexible and stiff steel building, obtained via solving the Bouc-Wen material model. $\{z\}$ matrix represents the hysteresis DOFs of the buildings. $\{F_{hf}\}$ and $\{F_{hs}\}$ are the damper force coming to the flexible and stiff buildings, obtained through solving Bouc-Wen model for yield damper and Graesser-Cozzarelli model for SMA damper. $\{r\}$ is influence coefficient vector and $\ddot{u}_g$ is input ground motion.

Response of the buildings under seismic excitation is obtained by solving the equation of motion of the coupled building system by step-by-step Newmark-beta (Average acceleration) integration method. Here, the buildings and dampers both are modelled to go into non-linear regime, and therefore the equation of motions with the non-linear material

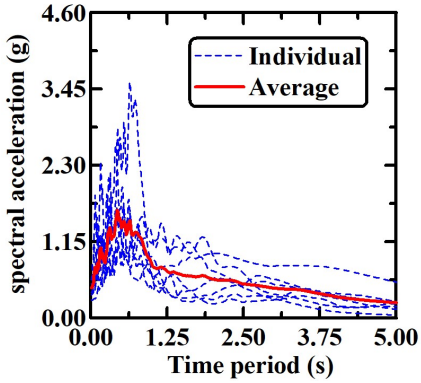


**Fig. 4:** Spectral acceleration of selected ground motions

models are solved iteratively considering a very small-time step i.e. $\Delta t = 0.0001$ s. For each time step, multiple iterations of solutions are performed to get the most accurate results. Iterations are performed until the difference between two consecutive solutions for iteration become less than a certain tolerance limit ($\delta_{tol} = 10^{-5}$). Damper parameters, building parameters and the values of $\Delta t$ and $\delta_{tol}$ are taken from relevant previous studies [19–21].

### *3.2 Ground motion selection*

Response output of dynamic analysis of any structure strongly depends on the characteristic of the input ground motion. Some of the very recent studies [19, 20, 22] already demonstrated that the traditional control system loses its control efficiency under near-fault ground motions, due to the presence of long-period and high-amplitude velocity pulses. Thus, possible coincident of the time period of velocity pulses and the controlled buildings can trigger the resonance phenomena, which ultimately can cause substantial damage to building structures. Therefore, a set of real pulse type earthquakes i.e. fault normal component of the ground motion with near fault characteristics are adopted for the numerical study. Fig. 4 shows the spectral acceleration of selected ground motions. Contrary to the non-pulse motions, pulse type ground motions have substantial peaks at higher durations, as mentioned in other study [23], also obtained in the spectral acceleration plots of this study, in Fig. 4. More details about the selected ground motion are available in the previous study [19–20, 24]. However, during the selection process of ground motion, consideration has been put to capture the wide range of variations in PGAs (from 0.35g to 0.90g) and dominant time period (0.28s to 0.84s).

## 4. Results and Discussion

This section provides the results of non-linear time history of unconnected and connected (via yield and SMA dampers) buildings. At first the response analysis has been performed to establish the superior control efficiency of SMA damper, followed by a detailed parametric study. For the simulation process, default value of different parameters are adopted. Flexible and stiff buildings' fundamental mode time period = 1.0 s and 0.5 s, respectively, damping ratio = 2.0 %, normalized yield strength of building column = 1.0, post-to-pre yielding stiffness ratio 0.02, and hysteresis loop parameters for the building column $\delta = 1.0, \gamma = \beta = 0.5$, and $\eta = 10.0$; for yield damper normalized yield strength = 0.1 with the yield displacement = 0.025 m, post-to-pre yielding stiffness ratio 0.05, and hysteresis loop parameters

$\delta = 1.0$, $\gamma = \beta = 0.5$, and $\eta = 1.0$; finally, for SMA damper normalized transformation strength of SMA = 0.125 with the transformation displacement = 0.035 m, post-to-pre yielding stiffness ratio 0.10, and hysteresis loop parameters $a = 2500$, $c = 0.001$, $f_T = 0.07$, and $\nu = 3.0$. Note that, the values of different parameters are adopted for previous studies [19–21]. Here for simulation purpose, a seven-storey non-linear steel building frame represents the flexible building and a five-storey non-linear steel building frame represents the stiff building. These buildings are first analysed in unconnected state and then in connected state. In connected state, the buildings are connected first with yield damper and then with SMA damper at alternate floor levels i.e., at 1st, 3rd and 5th floor levels.

At first the results of non-linear time history analysis is shown in Fig. 5 (for both unconnected and connected buildings), under Imperial Valley earthquake (10/15/1979 station and component ElCentro array #5, 230). Fig. 5 (a) and (b) shows the top floor acceleration and displacement of flexible building, and Fig. 5 (c) and (d) provides the response of top floor acceleration and displacement for stiff building. In case of flexible building, compare to the unconnected case, yield and SMA damper reduces top floor acceleration by 5.6 % and 16.5 %, respectively; whereas for the top floor displacement, the control (reduction) efficiency is 17.8 % for yield damper and 31.9 % for SMA damper. Similarly, for the stiff building, top floor acceleration reduction efficiency is 23.6 % for yield damper and 51.3 % for SMA damper. Subsequently, the top floor displacement of stiff building, yield and SMA dampers provided 10.2 % and 34.5 % reduction than uncontrolled case, respectively. Another very important observation is that the large residual displacement reduction efficiency of SMA damper over yield damper. Due to the re-centring capability of SMA material, at the of ground motion SMA damper connected buildings (both flexible and stiff) leaves almost no residual deformation. In comparison to the yield damper, SMA damper reduces the residual displacement by 81.7 % for flexible building and 43.3 % for stiff building. Fig. 5 (e) and (f) shows the bi-linear hysteresis loop of flexible and stiff building column, respectively, for unconnected and yield or SMA damper connected buildings. For the unconnected and yield damper connected buildings residual displacement is clearly observable, which is otherwise not present in case of SMA damper connected buildings. Fig. 5 (g) shows the force displacement hysteresis loop for the yield damper and SMA damper. Here also hysteresis loop of yield damper shows the large residual displacement, whereas SMA damper shows no residual displacement.

Next section provide the results of the parametric study to determine the vibration control efficiency of SMA and yield dampers for non-liner connected buildings. Here, numerical analysis are conducted with varying normalized strength of column and damper, frequency ratio of the stiff to the flexible building, fundamental time period of the flexible structure, peak ground acceleration, and predominant time period of the ground motion. As the response output, peak floor acceleration, peak floor displacement, and the residual displacement are calculated, under all seven ground motion records. Average values of all three output variables are presented here and compared for unconnected, yield damper connected and SMA damper connected building structures. Here it is important to note that, during parametric study at any time only one parameter has been changed and values of the other parameters are kept constant to their default value.

Previous literatures [19] suggested that, normalized strength of damper is an important design parameter for optimal vibration control of the connected buildings. Effect of varying normalized strength of dampers on the building responses is presented in Fig. 6 (a1)-(c1). Fig. 6 (a1) and (b1), which shows the lowest peak floor response (acceleration and displacement) in case of SMA damper connected flexible and stiff buildings, suggesting better control efficiency for SMA dampers than yield dampers. Also, with increase in the normalized strength of dampers, peak floor acceleration of stiff buildings and peak floor displacement of flexible building decreases. But the peak floor acceleration of the flexible buildings and the peak floor displacement of stiff building increases with increase in normalized strength of damper. Therefore, selection of the optimum normalized strength of dampers is necessary in controlling both the acceleration and the displacement responses of the flexible and stiff buildings simultaneously. Fig. 6 (c1) shows the maximum residual displacement of the buildings. SMA damper substantially reduced the residual displacement of flexible and stiff buildings, when compared with the unconnected and yield damper connected buildings. Thus the property of SMA to the recover residual strain is extremely beneficial in its application as passive damper as it helps reduce large permanent deformations in the structure at the end of a seismic event. Fig. 6 (a2)-(c2) shows the effect of normalized yield strength of building column on the peak floor acceleration, displacement, and residual displacement. Results from Fig. 6 (a2) depicts that, neither for the flexible building nor for the stiff building, yield damper does not provide sufficient reduction for peak floor acceleration, in comparison to the unconnected building. In contest to yield damper, SMA damper is much better of acceleration for both of the buildings. Fig. 6 (b2) shows the peak floor displacement control efficiency of the yield and SMA damper. For flexible building both of the damper (yield and SMA) shows good displacement reduction efficiency, with the higher control efficiency for SMA damper. However for stiff building, yield damper does not provide any noticeable reduction, whereas SMA damper shows good amount of displacement reduction. Fig. 6 (c2) clearly shows very high residual displacement reduction control efficiency for SMA damper (for the flexible building), over yield damper.

Next, the control efficiency of yield and SMA dampers is studied under varying frequency ratio of the stiff to the flexible building. Here, the frequency ratio refers to the ratio of the fundamental frequency of stiff building to that of the flexible building. The time period of flexible building is kept constant (i.e., 1 s) and time period of stiff building is varied making variation in the frequency ratio for the study. Changes in the fundamental time period of stiff buildings are made through changing the stiff building properties like floor mass and stiffness etc. For connecting buildings, frequency ratio is also one of the important parameter and its effect on building response is presented in Fig. 7 (a1)-(c1). Fig. 7 (a1) and (b1) shows the peak floor acceleration and displacement respectively, under the varying frequency ratio of buildings.

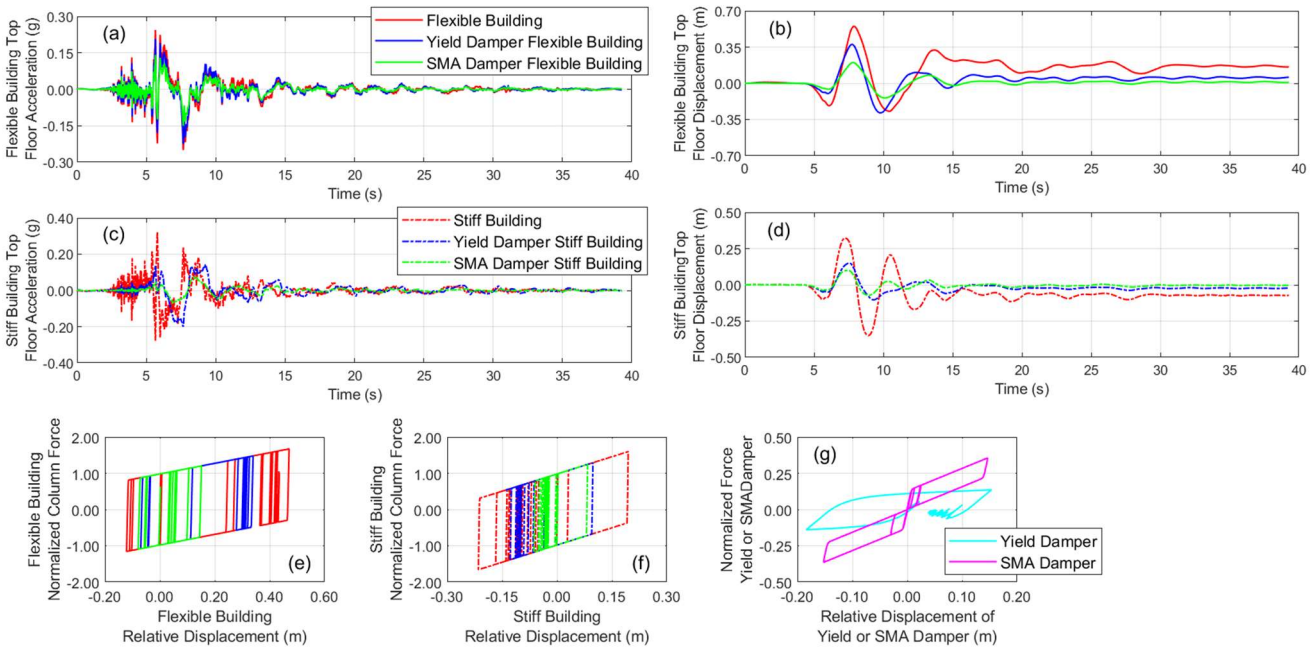


**Fig. 5:** Time history response results of flexible building top floor (a) acceleration, (b) displacement and stiff building top floor (c) acceleration (d) displacement without and with dampers under Imperial Valley earthquake (10/15/1979, station ElCentro array #5, 230). Force displacement hysteresis loop for (e) flexible and (f) stiff building column, and (g) yield and SMA damper.

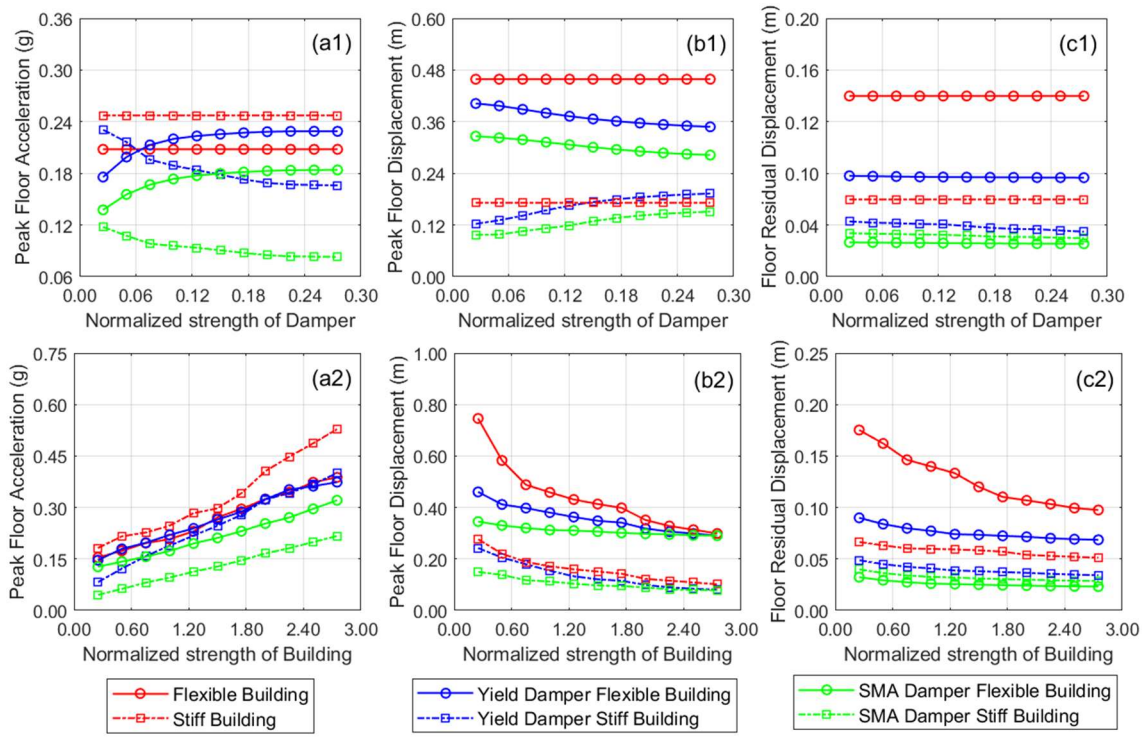


**Fig. 6:** Effect of variation of normalized strength of damper on (a1) peak floor acceleration, (b1) peak floor displacement, and (c1) floor residual displacement. Effect of variation of normalized strength of building column on (a1) peak floor acceleration, (b1) peak floor displacement, and (c1) floor residual displacement.

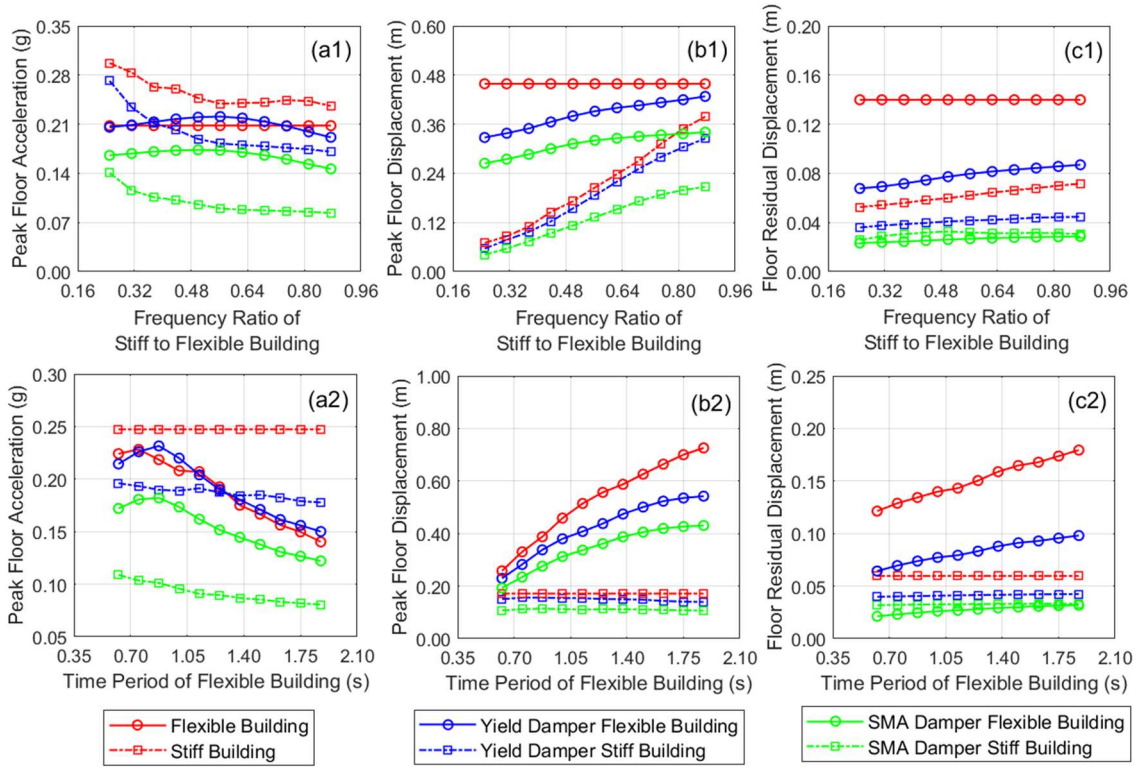


**Fig. 7:** Effect of variation of frequency ration of building (stiff to flexible) on (a1) peak floor acceleration, (b1) peak floor displacement, and (c1) floor residual displacement. Effect of variation of the time period of flexible building on (a1) peak floor acceleration, (b1) peak floor displacement, and (c1) floor residual displacement.

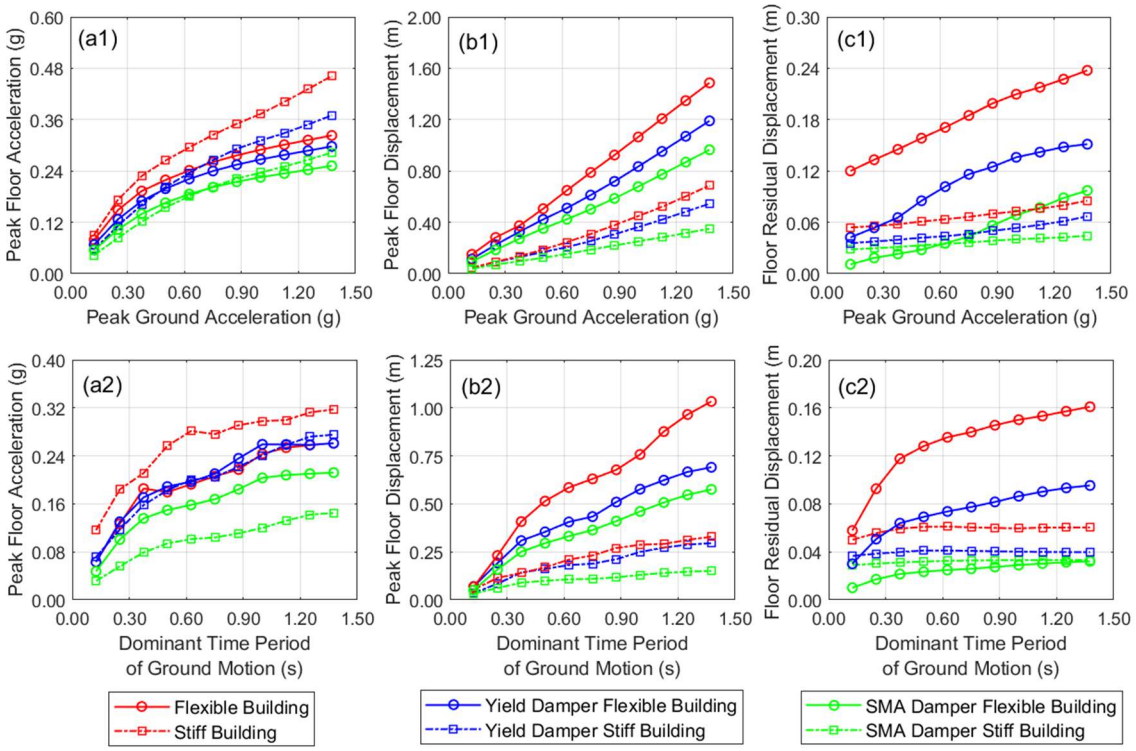


**Fig. 8:** Effect of variation of peak ground acceleration on (a1) peak floor acceleration, (b1) peak floor displacement, and (c1) floor residual displacement. Effect of variation of dominant time period of ground motion on (a1) peak floor acceleration, (b1) peak floor displacement, and (c1) floor residual displacement.

Similar to previous results, SMA damper connected buildings show lower responses than the yield damper connected building. The floor residual displacement under the varying frequency ratio is presented in Fig. 7(c) and its shows lowest residual displacement for SMA damper connected buildings.

For the next parametric analysis, flexible building period is varied keeping the stiff building's period constant. This study helps us to access the suitability of the dampers for connecting buildings with different time periods of flexible structure. Results (peak floor acceleration and displacement, and peak floor residual displacement) from the analysis are presented in Fig. 7 (a2)-(c2). Fig. 7 (a2) and (b2) present the peak floor acceleration and displacement with the varying time period of flexible building. With the increase in flexible building time period, acceleration response decreased and displacement response increased for flexible building. However the stiff building shows almost no (for unconnected case) or negligible (for yield or SMA damper connected case) variation. In case of the flexible building, yield damper shows almost no floor acceleration reduction than unconnected case, but provides noticeable level of floor displacement reduction efficiency. Considering different cases of the flexible and stiff buildings' (unconnected and connected via yield or SMA damper) response of the SMA damper connected building are the least among all. Fig 7 (c2) presents an important finding on the residual displacement control efficiency of the yield and SMA dampers. With increase in flexibility (flexible building's period) residual displacement of unconnected and the yield damper connected flexible building increased drastically, about 1.5 to 2.0 times, for a variation of just 1 s time period of structure. But it remained almost constant for SMA damper connected building, and it is also very low in comparison to the unconnected or yield damper connected flexible building. This observation suggests that, for flexible buildings, SMA dampers are far better than the yield damper as a vibration control device, in terms of recovering residual deformations after a seismic activity.

Finally the effect of ground motion intensity (PGA) and frequency content (dominant time period) scaling on the response output has been studied. Fig. 8 (a1)-(c1) shows the effect of ground motion intensity scaling i.e. peak ground acceleration (PGA) scale on the peak floor acceleration, peak floor displacement, and residual displacement, respectively. Aligning with the previous results, SMA damper connected flexible and stiff buildings shows lower values of peak floor acceleration and displacements under the varying values of PGA, when compared with the unconnected and yield damper connected buildings. Interestingly, at the lower PGA values, responses of unconnected building, yield damper connected and SMA damper connected buildings are comparable. But with the increasing PGA values, superior control efficiency of the SMA dampers in response reduction is quite significant and as well as clearly observable. Next, Fig. 8 (c1) shows the variation residual floor displacement under varying PGA values. As it can be observed, with increasing PGA values, residual floor displacement of unconnected flexible buildings increases significantly, and also for yield damper connected buildings. However, due to the better re-centering capability of the superelastic SMA material, SMA damper connected flexible building shows only a marginal increase in floor residual displacement, even at higher PGA values. In case of stiff building, compare to unconnected case, both yield and SMA damper provides sufficient reduction in the residual floor displacement.

An ideal damper should behave efficiently under seismic excitations with wide range of dominant frequency content or time periods in ground motion. Therefore, to access the control efficiency of SMA and yield damper with varying dominant time period of the ground motions, numerical simulation is conducted and the obtained building responses are presented in Fig. 8 (a2)-(c2). Fig 8 (a2) and (b2) shows the peak floor acceleration and displacement responses, respectively; for the flexible and stiff buildings with SMA and yield dampers, as well as for unconnected building. Analysis shows a monotonic increase in floor responses in all the considered cases, with bumps showing local maxima at the fundamental time period of flexible (1 s) and stiff (0.5 s) buildings, with the increase in the dominant time period of excitations. Here also, compare to the unconnected building, yield dampers shows almost no reduction in the peak floor acceleration for the flexible building and good reduction for stiff building. In case of peak floor displacement control efficiency, noticeable reduction (than unconnected case) can be observed for the yield damper connected flexible building, however for the stiff building it shows almost same peak floor displacement. Comparing the performance of yield and SMA damper connected building, SMA connected buildings (both flexible and stiff) show the least increase in the peak floor acceleration and displacement, with increase in the dominant time period of ground motion. Fig. 8(c2) shows the peak value of residual floor displacement for the unconnected and yield or SMA damper connected buildings (both flexible and stiff), under varying dominant time period of ground motion. Unconnected and yield damper connected flexible buildings show significant level of residual displacement, however SMA damper shows large reduction (almost 2.0 to 2.5 times). For stiff building, in contrast to the unconnected building, yield and SMA damper connected building shows similar level of variation in residual displacement. Thus it is clear that, compare to yield damper, SMA damper provided superior control efficiency.

## 4. Conclusion

Efficiency of conventional yield dampers and a new SMA dampers as the passive vibration control device in non-linear coupled building frame systems are studied her. Yield and SMA dampers are modelled using Bouc-Wen and Graesser-Cozzarelli material models, respectively. For the response analysis using a set of seven near-fault type past ground motions, non-linear dynamic time history analyses are conducted. As the response output, peak floor acceleration, peak floor displacement and residual displacement are estimated compared to unconnected, and yield and SMA damper connected buildings. Time history analysis shows better control efficiency of superelastic SMA dampers over yield dampers. Hysteresis loop of yield damper shows good energy dissipation capacity but leaves large residual strain, whereas smart SMA dampers has hysteresis loop with dual

advantages: (a) flag-shaped hysteresis loops with better energy dissipation and (b) negligible residual deformation. These added benefits of hysteresis loop of SMA dampers are visible in its improved response control as a passive damper. Further, SMA damper connected nonlinear buildings shows simultaneous reduction in acceleration of stiff building and displacement of flexible buildings, and this is most desirable conditions for the vibration control of connected buildings.

Next, superior control efficiency of SMA dampers over yield dampers is examined under varying characteristic damper parameters, building structure parameters, and ground motion parameters. Compared to the yield damper, SMA damper shows 13 % to 25 % less peak floor acceleration for the flexible building, and in case of stiff building the peak floor acceleration is reduced by 23 % to 56 %. For peak floor displacement control efficiency, in comparison to the yield damper, SMA damper provides 2 % to 29 % reduction for flexible building and 7 % to 47 % reduction for flexible building. Finally, SMA damper acts as much better re-centering device and leaves very less residual displacement. Compare to yield damper, SMA damper reduces the residual floor displacement by 36 % to 64 % for flexible building and by 15 % to 34 % for stiff building. All of the above findings suggest SMA as a better material for the passive vibration control devices with good energy dissipation capacity, better acceleration and displacement control efficiency and almost no or negligible residual displacement.

**Acknowledgment**

Financial support provided by the Department of Science and Technology (DST) of the Government of India, through the Start-up Research Grant (SRG/2020/000892) by the Science and Engineering Research Board (SERB) is acknowledged.



**References**

1. Patel CC, Jangid RS. Seismic response of adjacent structures connected with maxwell dampers. Asian Journal of Civil Engineering, 2010; 11(5): 585–603.
2. Bhaskararao AV, Jangid RS. Seismic response of adjacent buildings connected with friction dampers. Bulletin of Earthquake Engineering, 2006; 4: 43–64.
3. Bhaskararao AV, Jangid RS. Harmonic response of adjacent structures connected with a friction damper. Journal of Sound and Vibration, 2006; 292(3–5): 710–725.
4. Matsagar VA, Jangid RS. Viscoelastic damper connected to adjacent structures involving seismic isolation. Journal of Civil Engineering and Management, 2005; 11(4): 309–322.
5. Ying ZG, Ni YQ, Ko JM. Stochastic optimal coupling-control of adjacent building structures. Computers and Structures, 2003; 81(30–31): 2775–2787.
6. Ni YQ, Ko JM, Ying ZG. Random seismic response analysis of adjacent buildings coupled with non-linear hysteretic dampers. Journal of Sound and Vibration, 2001; 246(3): 403–417.
7. Ge DD, Zhu HP, Wang DS, Huang MS. Seismic response analysis of damper–connected adjacent structures with stochastic parameters. Journal of Zhejiang University Science A, 2010; 11: 402–414.
8. Takewaki I. Earthquake Input Energy to Two Buildings Connected by Viscous Dampers. Journal of Structural Engineering, 2007; 133(5): 620–628.
9. Moreschi LM, Singh MP. Design of yielding metallic and friction dampers for optimal seismic performance. Earthquake Engineering and Structural Dynamics, 2003; 32(8): 1291–1311.
10. Bhaskararao AV, Jangid RS. Optimum viscous damper for connecting adjacent SDOF structures for harmonic and stationary white-noise random excitations. Earthquake Engineering and Structural Dynamics, 2007; 36(4): 563–571.
11. Matsagar VA, Jangid RS. Base-isolated building connected to adjacent building using viscous dampers. Bulletin of the New Zealand Society for Earthquake Engineering, 2006; 39(1): 59–80.
12. Patel CC, Jangid RS. Optimum Parameter of Viscous Damper for Damped Adjacent Coupled System. Journal of Civil Engineering and Science, 2012; 1(1): 22–30.
13. Palermo M, Silvestri S. Damping reduction factors for adjacent buildings connected by fluid-viscous dampers. Soil Dynamics and Earthquake Engineering, 2020; 138: 106323.
14. Lu L, Xu J, Zhou Y, Zhou Y, Lu W, Spencer BF. Viscous inertial mass damper (VIMD) for seismic responses control of the coupled adjacent buildings. Engineering Structures, 2021, 233: 111876.
15. Ozbulut OE, Hurlebaus S, Desroches R. Seismic Response Control Using Shape Memory Alloys: A Review. Journal of Intelligent Material Systems and Structures, 2011; 22:1531–1549.
16. Parulekar YM, Reddy GR, Vaze KK, Gupta S, Gupta C, Muthumani K, Sreekala R. Seismic response attenuation of structures using shape memory alloy dampers. Structural Control and Health Monitoring, 2012; 19(1): 102–119.
17. Wen YK. Equivalent linearization for hysteretic systems under random excitation. Journal of Applied Mechanics, Transactions ASME, 1980; 47(1): 150–154.
18. Graesser EJ, Cozzarelli FA. Shape-memory alloys as new materials for aseismic isolation. Journal of Engineering Mechanic, 1991; 117(11): 2590–2608.
19. Gur S, Singh P, Roy K. Seismic response of adjacent building structure connected with superelastic damper: comparison with yield damper. EURODYN 2020, Proceedings of XI International Conference on Structural Dynamics, 2020; 4696–4709.
20. Gur S, Xie Y, DesRoches R. Seismic fragility analyses of steel building frames installed with superelastic shape memory alloy dampers: Comparison with yielding dampers. Journal of Intelligent Material Systems and Structures, 2019; 30 (18–19): 2670–2687.

21. Gur S, Mishra SK, Roy K. Stochastic seismic response of building with super-elastic damper. Mechanical Systems and Signal Processing, 2016; 72–73: 642–659.

22. Gur S, Mishra SK, Chakraborty S. Performance assessment of buildings isolated by shape-memory-alloy rubber bearing: comparison with elastomeric bearing under near-fault earthquakes. Structural Control and Health Monitoring, 2014; 21(4): 449–465.

23. Saha A, Mishra SK. Amplification of seismic demands in inter-storey-isolated buildings subjected to near fault pulse type ground motions. Soil Dynamics and Earthquake Engineering, 2021; 147: 106771.

24. Gur S, Frantziskonis GN, Mishra SK. Thermally modulated shape memory alloy friction pendulum (tmSMA-FP) for substantial near-fault earthquake structure protection. Structural Control and Health Monitoring, 2017; 24(11): e2021.